CLASSICAL AND QUANTUM MECHANICS
OF A STRONGLY CHAOTIC BILLIARD SYSTEM*

M. SIEBER and F. STEINER
II. Institut für Theoretische Physik, Universität Hamburg, Luruper Chaussee 149, D-2000 Hamburg 50, Fed. Rep. Germany

We study the hyperbola billiard, a strongly chaotic system whose classical dynamics is the free motion of a particle within the region $D = \{(x, y)|x \geq 0 \wedge y \geq 0 \wedge y \leq 1/x\}$ with elastic reflections on the boundary ∂D. The corresponding quantum mechanical problem is to determine the bound state energies as eigenvalues of the Dirichlet Laplacian on D. It is shown that the classical periodic orbits of the hyperbola billiard can be effectively enumerated by a ternary code. Combining this code with an extremum principle, we are able to determine with high precision more than 500 000 primitive periodic orbits together with their lengths, multiplicities and Lyapunov exponents. The statistical properties of the length spectrum of the periodic orbits are found to be consistent with a random walk model, which in turn predicts asymptotically an exponential proliferation of long periodic orbits and leads to a novel formula for the topological entropy τ, whose value turns out to be approximately 0.6. The periodic orbits are used for a quantitative test of Gutzwiller's periodic-orbit theory, which plays the role of a semiclassical quantization rule. We find that the predictions of the periodic-orbit theory for the Gaussian level density agree at low energies surprisingly well with the "true" results obtained from a numerical solution of the Schrödinger equation.

1. Introduction

Despite the early recognition of chaotic motion in nature by Poincaré and Hadamard at the end of the nineteenth century, detailed studies of "deterministic chaos" have only been carried out in the last few decades. Today, however, our knowledge of classically chaotic systems is very rich, and most natural scientists slowly appreciate the important role played by chaos in nonlinear dynamical systems. On the other hand, the question how classical chaos manifests itself in quantum mechanics, has attracted only recently the attention of more than a few pioneers. The only known, commonly accepted quantitative theory aiming at unravelling the mystery of "quantum chaos" is based just on the earliest approach, namely the semiclassical approximation of the Feynman path integral pioneered by Gutzwiller [1] (see also refs. [2, 3]).

The standard semiclassical quantization rules of Bohr–Sommerfeld–Einstein–WKB type are based on the assumption that phase space is divided into invariant tori. In this case the path integral can be approximated by a sum over all classical trajectories which wind on the invariant tori. But for chaotic or

non-integrable systems it is well known that phase space has a much more complicated structure and thus the standard semiclassical quantization rules cannot be applied. What is required instead is a substitute for these quantization rules for chaotic systems. Gutzwiller's periodic-orbit theory provides this substitute. In this theory the path integral is replaced by an infinite sum over all periodic orbits, i.e. the quantum mechanical energy spectrum is determined by purely classical quantities like the periods or lengths of the unstable periodic orbits and their Lyapunov exponents.

Although Gutzwiller's approximation amounts to a tremendous simplification of the path integral for chaotic systems by replacing a very complicated functional integral by an ordinary sum over classical trajectories, we are still facing another extremely complicated problem, now in classical mechanics, namely the enumeration of the periodic orbits and the calculation of their lengths and Lyapunov exponents. In contrast to integrable systems, where the number of periodic orbits increases only like a power law, for chaotic systems the number of periodic orbits whose lengths are smaller than a given length increases exponentially. The exponential proliferation of long periodic orbits implies that a successful application of the periodic-orbit theory can only be expected, if enough periodic orbits together with their lengths and Lyapunov exponents are explicitly known for a given non-integrable system. Thus it is mandatory to have an effective method at hand which allows us to determine in a systematic way the shortest periodic orbits.

Until recently the only quantitative test of the periodic-orbit theory for strongly chaotic systems was carried out by Gutzwiller for the anisotropic Kepler problem [4]. Only within the last few years a few other systems have been investigated [5]. However, in most of the cases people were not able to give a systematic enumeration of a large number of periodic orbits. There is a very special system, namely the Hadamard–Gutzwiller model [6], for which millions of periodic orbits could be calculated [7, 8] by using very powerful results from the theory of compact Riemann surfaces and Fuchsian groups, and an effective algorithm implemented on a large computer.

In view of this situation it seems worthwhile to look for other dynamical systems, which are classically chaotic but yet simple enough to allow an explicit enumeration of a large number of periodic orbits. It is the purpose of this paper to present the results of a detailed study of an example of the simplest kind of chaotic systems, namely a two-dimensional plane billiard system, which we call *hyperbola billiard*, whose domain is given by

$$D := \{(x, y) | x \geq 0 \wedge y \geq 0 \wedge y \leq 1/x\}, \tag{1}$$

i.e. the area bounded by the x-axis, the y-axis and the hyperbola $y = 1/x$. The quantum-mechanical problem is to find the eigenvalues and eigenfunctions of the Laplace operator on D with the condition that the wave functions vanish on the boundary of the billiard region (Dirichlet problem). The corresponding classical motion is the free motion of a particle with mass m within the billiard area with elastic reflections on the boundary. This motion is strongly chaotic in virtue of the fact that neighbouring trajectories separate exponentially. All periodic orbits are unstable and have an instability exponent greater than zero (see appendix B).

There are two crucial points which enable us to give an effective enumeration of the periodic orbits of the hyperbola billiard:

(i) In section 2.1 we show that there exists an efficient classification of the periodic orbits in terms of a ternary code, i.e. the set of all periodic orbits is represented by the set of words formed by three letters obeying a certain grammar.

(ii) It is a characteristic feature of chaotic systems, that their evolution in time depends sensitively on the initial conditions, since neighbouring trajectories diverge exponentially in time. It thus seems impossible to determine the precise reflection points on the billiard boundary for a particle travelling on a long periodic orbit in our hyperbola billiard. We show, however, in appendix A that there exists an "extremum principle for periodic orbits" which allows us to get around this problem. The point is that all periodic orbits have the property that their length is minimal within a certain class of neighbouring "trial" trajectories that do not satisfy the elastic reflection condition on the hyperbolic boundary. Using this extremum principle we were able to find more than 500 000 primitive periodic orbits.

Our paper is organized as follows. In section 2.1 the coding of the periodic orbits and their symmetry properties are discussed. In section 2.2 we study several properties of the length spectrum of the periodic orbits. It is shown that the length spectrum proliferates exponentially, as expected, from which we infer for the topological entropy $\tau \approx 0.60$. It turns out that the distribution of lengths of all periodic orbits which are reflected N times on the hyperbola obeys for large enough N a universal law which is well described by a Gaussian. In section 3 we describe our numerical solution of the Schrödinger equation using the Rayleigh–Ritz method. The spectral staircase calculated from the approximate eigenvalues is at low energies well described by a modified Weyl's law. In section 4.1 the periodic orbits are used as an input in the periodic-orbit theory. Using a Gaussian smearing of the energy-level density, we are able to determine the lowest bound state energies. In order to increase the energy resolution of the periodic-orbit theory, we have desymmetrized the hyperbola billiard. In section 4.2 we discuss the application of the periodic-orbit theory to the two desymmetrized systems satisfying Dirichlet and Neumann boundary conditions on the line $y = x$, respectively. As expected, the energy resolution is significantly improved. Section 5 gives a discussion of our results. In appendix A the extremum principle for the periodic orbits is derived, and in appendix B the general form of the monodromy matrix is given.

2. Periodic orbits

2.1. Coding of the periodic orbits

It is possible to introduce an efficient classification for the periodic orbits of the hyperbola billiard. This will be explained in the following. A primitive periodic orbit is traversed once, and the number of reflections on the hyperbola is counted. Let this number be N. The N points on the hyperbola divide the orbit into N segments. Each segment is denoted by one of the three letters "x", "y" or "b" according to whether the particle is reflected in the segment on the x-axis only, on the y-axis only or on both axes, respectively (see appendix A). In this way to each periodic orbit is associated a ternary sequence of the form

$$a = (a_1, \ldots, a_N), \quad \text{where } a_i = \text{x, y or b.} \tag{2}$$

If for a given periodic orbit a different starting point on the hyperbola is chosen, we arrive at a ternary sequence which is a cyclic permutation of the original one. Therefore, if a sequence "a" is associated to a periodic orbit, every cyclic permutation of this sequence belongs to the same orbit. Examples are given in figs. 1a to 1e. The sequences are given for those starting points on the hyperbola which have the highest y value.
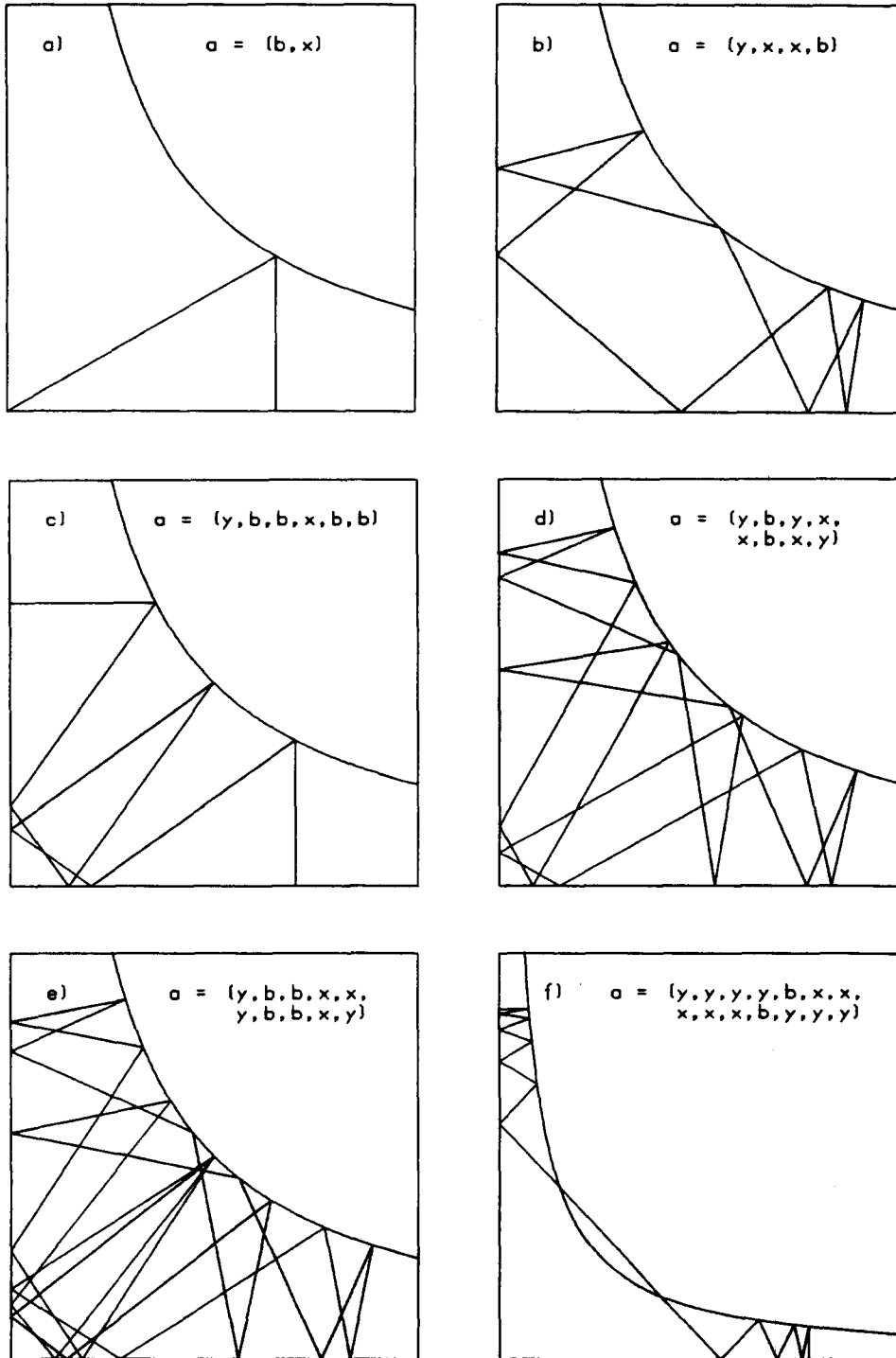
Fig. 1. (a) to (e) Examples of periodic orbits. (f) Forbidden periodic orbit.

The main point now is that extensive numerical investigations for $N = 1$ to 7 showed that there exists exactly one periodic orbit for every sequence. The only exceptions are sequences which consist of letters "x" only or of letters "y" only for which no periodic orbits exist. This fact and the extremum principle discussed in appendix A make it possible to search systematically for every single periodic orbit. If one wants to find the periodic orbit which is coded by a given sequence "a", one just has to form the length function $L(x_1, \ldots, x_N)$ which corresponds to this sequence (see appendix A) and to look for its minimum. Since there exist very efficient generalized Newton methods for finding the minimum of a given function, this is a very fast and accurate way to determine the periodic orbits. Using this method we were able to find more than 100 000 different primitive periodic orbits within two hours of computer time on an IBM 3084 with an accuracy of 16 significant digits.

The code can also be used to determine possible symmetries of a periodic orbit. For this purpose the ternary sequences are divided into classes, which we call *cyclic classes*. Two sequences "a" and "$\bar{a}$" belong to the same cyclic class if one is a cyclic permutation of the other:

$$a \equiv \bar{a} \Leftrightarrow a_i = \bar{a}_{i+n} \quad \forall i = 1, \ldots, N \quad \text{for } n \in \{1, \ldots, N\}. \tag{3}$$

Here we defined $a_{j+N} := a_j$. A given cyclic class therefore consists of all sequences which describe the same orbit. If a periodic orbit is geometrically reflected on the straight line $y = x$ one gets another periodic orbit since the system is invariant under the reflection R on this line. The sequence belonging to the reflected orbit, "Ra", is obtained from the sequence of the original orbit "a" by replacing all "x" by "y" and all "y" by "x":

$$Ra := \bar{a} \quad \text{where } \bar{a}_i = x \quad \text{if } a_i = y,$$

$$\bar{a}_i = y \quad \text{if } a_i = x,$$

$$\bar{a}_i = b \quad \text{if } a_i = b,$$

$$i = 1, \ldots, N. \tag{4}$$

An orbit is invariant under this reflection if $Ra \equiv a$ holds.

Another possible symmetry of an orbit is time-reversal. If an orbit is traversed in reverse direction, the sequence of the reversed orbit, "Ta", is the reverse sequence of the original orbit:

$$Ta := \bar{a} \quad \text{where } \bar{a}_i = a_{N+1-i}, \quad i = 1, \ldots, N. \tag{5}$$

An orbit is invariant under time-reversal, if $Ta \equiv a$ holds. In figs. 1a to 1e examples for all possible symmetries of a periodic orbit are given: (a) $a \equiv Ta \not\equiv Ra \equiv RTa$, (b) $a \not\equiv Ta \not\equiv Ra \not\equiv a \not\equiv RTa$, (c) $a \equiv Ta \equiv Ra \equiv RTa$, (d) $a \equiv Ra \not\equiv Ta \equiv RTa$, (e) $a \equiv RTa \not\equiv Ra \equiv Ta$.

Different orbits which are related by reflection or/and time-reversal give an identical contribution to the periodic-orbit theory. It is therefore useful to combine different cyclic classes to a bigger class, which we call *symmetry class*, if their sequences can be transformed into each other under reflection or/and time-reversal. To each symmetry class a multiplicity is associated which counts the number of different cyclic classes which are contained in it. This number can be 1, 2 or 4. It then suffices to determine one periodic orbit for each symmetry class.

If a sequence consists of identical partial sequences, for example

$$a = \left(\underbrace{x,x,y,b}, \underbrace{x,x,y,b}, \underbrace{x,x,y,b} \right),$$ (6)

it does not belong to a primitive orbit, but to an orbit which is traversed repeatedly. A class which belongs to a primitive orbit is called a primitive class. The number $Z(N)$ of primitive classes of sequences which consist of N letters satisfies the recursion relation

$$Z(N) = \frac{1}{N} \left(3^N - \sum_{\substack{M \mid N \\ M < N}} M \cdot Z(M) - 2 \right),$$ (7)

where we have taken into account that there are no periodic orbits for the sequences (x) and (y). The sum runs over all integers M that are divisors of N excluding $M = N$. The primitive periodic orbits for $N = 1$ to 14 were determined numerically. A number of $\sum_{N=1}^{14} Z(N) = 533\,828$ primitive periodic orbits was expected corresponding to 136 719 different primitive symmetry classes. But only for 136 699 symmetry classes periodic orbits could be found. Although for the remaining 20 forbidden symmetry classes a minimum of the length function $L(x_1, \ldots, x_N)$ could be found, the corresponding orbits cross the hyperbola like in fig. 1f. It is expected that the number of forbidden periodic orbits increases with increasing N.

2.2. Properties of the length spectrum of the periodic orbits

In figs. 2a and 2b the number $\mathcal{N}(l)$ of the determined orbits with lengths smaller or equal than l is shown,

$$\mathcal{N}(l) := \#\{\text{primitive periodic orbits } \gamma \text{ with length } l_\gamma \le l\}.$$ (8)

The expected asymptotic exponential proliferation of periodic orbits for chaotic systems, $\mathcal{N}(l) \sim e^{\tau l}/\tau l$, $l \to \infty$, is well confirmed in the region where the orbits were determined. A value of $\tau \approx 0.60$ was
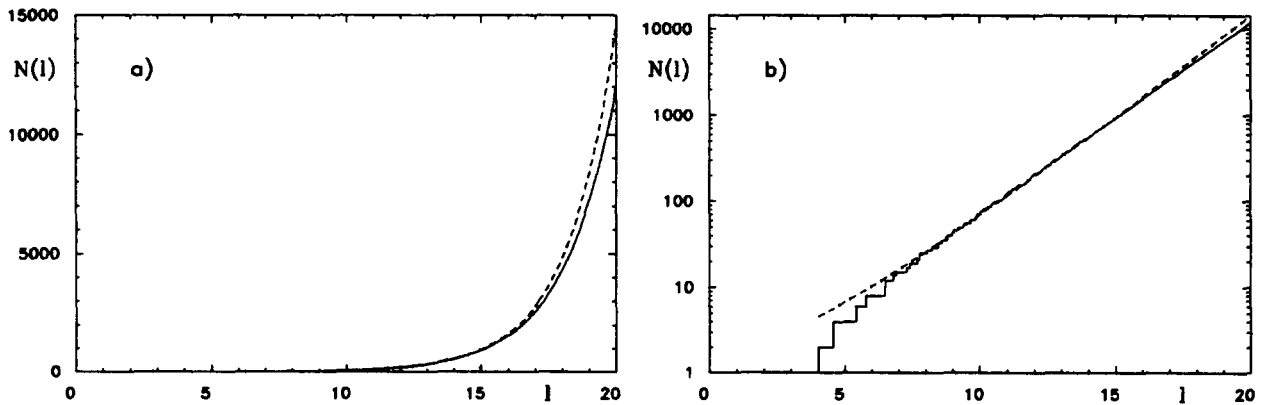

Fig. 2. The staircase function $\mathcal{N}(l)$ in comparison with the asymptotic law $e^{\tau l}/\tau l$ for $\tau = 0.6$ (dashed line); (a) linear scale, (b) logarithmic scale

obtained for the topological entropy τ from a fit in the region $10 < l < 15$, where the number of the periodic orbits is expected to be almost complete. Above $l \approx 15$ the calculated staircase function is below the curve corresponding to the asymptotic law $e^{\tau l}/\tau l$, see fig. 2. This is due to the fact that the contribution of periodic orbits which are reflected 15 times or more on the hyperbola is missing.

We also examined the distribution of lengths $p_N(l)$ of all periodic orbits which are reflected N times on the hyperbola along one traversal of the periodic orbit for $N = 1$ to 14. $p_N(l)\,\mathrm{d}l$ is the probability that a randomly chosen orbit with N reflections on the hyperbola will have a length between l and $l + \mathrm{d}l$. The result for $N = 14$ is shown in fig. 3a. It was found that the length distributions can be approximated very well by Gaussian curves if N is large enough ($N \geq 8$)

$$p_N(l) \approx \frac{1}{\sqrt{2\pi}\,\sigma_N} \exp\left(-\frac{(l - \bar{l}_N)^2}{2\sigma_N^2} \right),$$ (9)

where the mean value $\bar{l}_N$ and the standard deviation σ_N satisfy the relations

$$\bar{l}_N \approx \bar{l}N, \quad \bar{l} = 2.027,$$

$$\sigma_N \approx \sigma\sqrt{N}, \quad \sigma = 0.682.$$ (10)

In order to demonstrate this behaviour, we plotted $p_N(l + N\bar{l})/p_N(N\bar{l})$ as a function of $l/\sigma\sqrt{N}$ for $N = 10$ to $N = 14$ in fig. 3b. As can be seen there is good agreement between the length distributions that correspond to different values of N.

These results seem to indicate that the statistical properties of the length distributions can be described by a model in which the lengths of the orbits are the result of a random walk process with N independent steps where the displacements of each step have a mean value $\bar{l}$ and a standard deviation σ. This is also confirmed by an examination of the distribution of spacings $P(S)$ between adjacent lengths. $P(S)\,\mathrm{d}S$ is the probability that the spacings of a randomly chosen pair of neighbouring lengths will be between S and $S + \mathrm{d}S$, where S is measured as a fraction of the mean length difference $\overline{\Delta l}$ at the length considered: $S = \Delta l / \overline{\Delta l}$. In fig. 4 the result for $P(S)$ is plotted and compared to the Poisson distribution $P(S) = e^{-S}$. The agreement is excellent, which means that the lengths are uncorrelated.
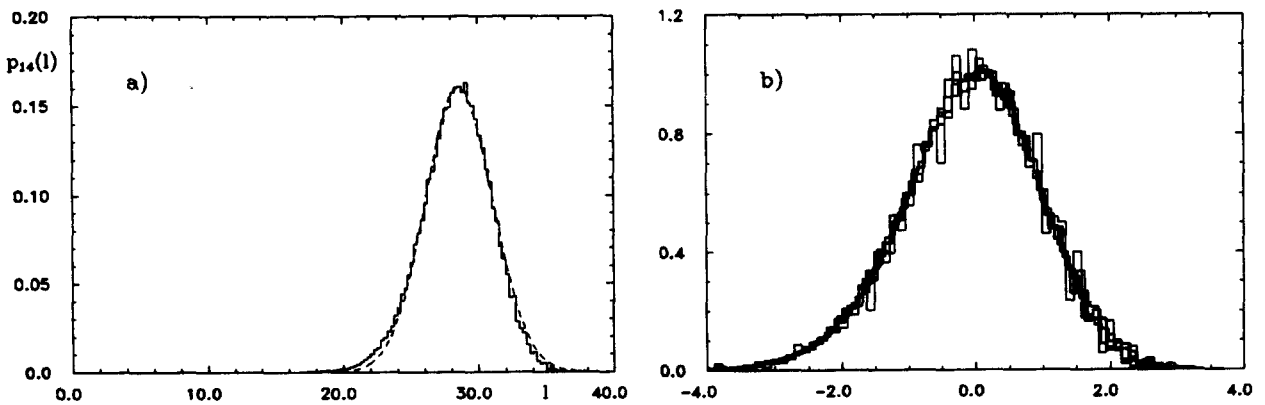

Fig. 3. (a) The length distribution $p_{14}(l)$ in comparison with a Gaussian. (b) Scaled length distributions $p_N(l + \bar{l}N)/p_N(\bar{l}N)$ as a function of $l/\sigma\sqrt{N}$ for $N = 10$ to $N = 14$.
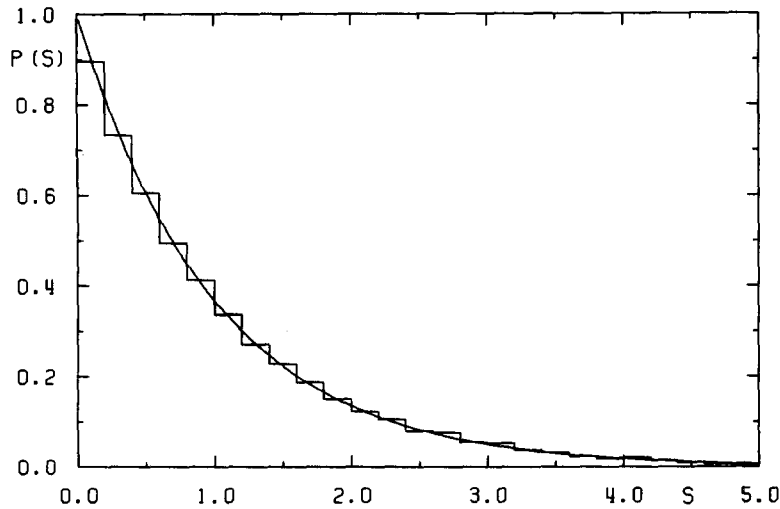
Fig. 4. Length spacings distribution $P(S)$.

The explicit dependence on N of the approximated length distributions $p_N(l)$, eq. (9), makes it possible to examine the asymptotic behaviour of the staircase function $\mathscr{N}(l)$ analytically:

$$\frac{d\mathscr{N}(l)}{dl} = \sum_{N=1}^{\infty} p_N(l) Z(N) \approx \sum_{N=1}^{\infty} \frac{1}{\sqrt{2\pi N}\,\sigma} \exp\left(-\frac{(l-\bar{l}N)^2}{2\sigma^2 N}\right) \frac{3^N}{N}. \tag{11}$$

A stationary phase approximation of this sum for large values of l yields the following result:

$$\frac{d\mathscr{N}(l)}{dl} \approx \frac{1}{l} \exp\left(\frac{l}{\sigma^2}\left(\bar{l} - \sqrt{\bar{l}^2 - 2\sigma^2 \log 3}\right)\right), \quad l \gg 1. \tag{12}$$

A comparison with the expected asymptotic behaviour $d\mathscr{N}/dl \approx e^{\tau l}/l$, $l \to \infty$, leads to an explicit expression for the *topological entropy* of the form

$$\tau = \frac{1}{\sigma^2}\left(\bar{l} - \sqrt{\bar{l}^2 - 2\sigma^2 \log 3}\right). \tag{13}$$

The numerical value $\tau \approx 0.58$ which is obtained from this equation is in good agreement with the previously obtained value $\tau \approx 0.6$.

The Lyapunov exponents of the periodic orbits were determined using the method of appendix B. In fig. 5 the Lyapunov exponents λ_γ are plotted as a function of the orbit lengths l_γ (for fixed energy $E = m/2$).
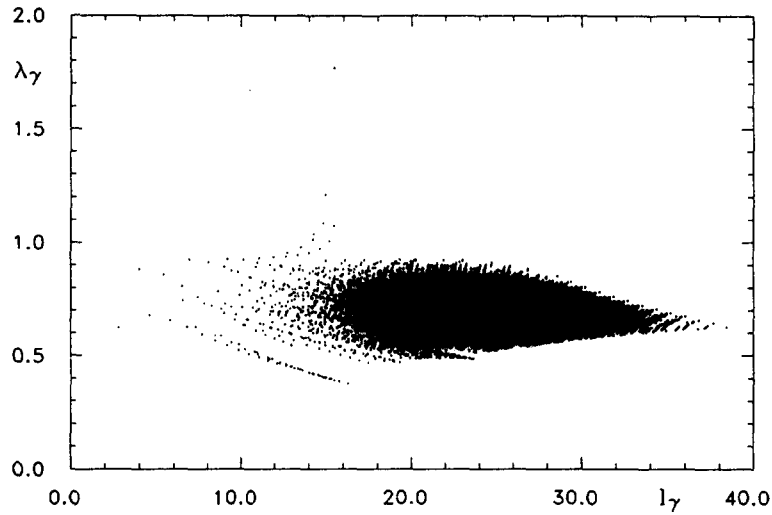
Fig. 5. Lyapunov exponents λ_γ in dependence on orbit lengths l_γ.

3. The energy spectrum

The quantal energies E_n are determined by the *Schrödinger equation* ($\hbar = 2m = 1$)

$$-\left(\frac{\partial^2}{\partial x^2} + \frac{\partial^2}{\partial y^2} \right) \Psi_n(x,y) = E_n \Psi_n(x,y), \quad (x,y) \in D, \tag{14}$$

with Dirichlet boundary conditions

$$\Psi_n(x,y) = 0 \quad \text{if } x = 0 \text{ or } y = 0 \text{ or } y = 1/x. \tag{15}$$

Introducing hyperbolic coordinates

$$\begin{aligned} \eta &= xy, & 0 \le \eta \le 1, \\ \xi &= \tfrac{1}{2}(x^2 - y^2), & -\infty < \xi < +\infty, \end{aligned} \tag{16}$$

eq. (14) transforms into

$$-2\sqrt{\eta^2 + \xi^2} \left(\frac{\partial^2}{\partial \eta^2} + \frac{\partial^2}{\partial \xi^2} \right) \psi_n(\eta, \xi) = E_n \psi_n(\eta, \xi) \tag{17}$$

with boundary conditions

$$\psi_n(\eta, \xi) = 0 \quad \text{if } \eta = 0 \text{ or } \eta = 1. \tag{18}$$

The first energy eigenvalues were numerically determined using the Rayleigh–Ritz method. This method is based on a variational principle which yields upper bounds for the energy eigenvalues. An approximate

solution of eq. (17) of the form

$$\psi_n(\eta,\xi) = \sum_{m=1}^{M} a_m^n \varphi_m(\eta,\xi)$$ (19)

is sought for with suitable functions $\varphi_m(\eta,\xi)$ that are linearly independent and satisfy the boundary conditions eq. (18). The minimum principle of Rayleigh then leads to the eigenvalue problem

$$\sum_{j=1}^{M} (A_{ij} - \mu_n B_{ij}) a_j^n = 0, \quad i, n = 1, \dots, M,$$ (20)

where

$$A_{ij} = \int_{-\infty}^{+\infty} \mathrm{d}\xi \int_0^1 \mathrm{d}\eta \left(\frac{\partial}{\partial\eta} \varphi_i(\eta,\xi) \frac{\partial}{\partial\eta} \varphi_j(\eta,\xi) + \frac{\partial}{\partial\xi} \varphi_i(\eta,\xi) \frac{\partial}{\partial\xi} \varphi_j(\eta,\xi) \right)$$ (21)

and

$$B_{ij} = \int_{-\infty}^{+\infty} \mathrm{d}\xi \int_0^1 \mathrm{d}\eta \frac{\varphi_i(\eta,\xi)\varphi_j(\eta,\xi)}{2\sqrt{\eta^2 + \xi^2}}.$$ (22)

The eigenvalues μ_n of eq. (20) are upper bounds for the first M energies E_n. The functions $\varphi_m(\eta,\xi)$ were chosen to be products of sine-functions in the η-direction and eigenfunctions of the one-dimensional harmonic oscillator in the ξ-direction. Altogether 200 different functions $\varphi_m(\eta,\xi)$ were used. The result for the first ten energy eigenvalues is listed in table 1.

In fig. 6 the spectral staircase function

$$N(E) = \#\{E_n | E_n \leq E\}$$ (23)

is shown for $0 \leq E \leq 100$. It should asymptotically obey a *modified Weyl's law* [9]

$$N(E) \sim \frac{1}{4\pi} E \log E + \frac{a}{4\pi} E + \frac{b}{4\pi} \sqrt{E} + \dots, \quad E \to \infty$$

$$a = 2(\gamma - \log 2\pi) = -2.5213,$$

$$b = 4\pi^{3/2}/\Gamma^2(1/4) = 1.6944.$$ (24)

This curve is also shown in fig. 6. As can be seen, the asymptotic law is a good approximation to the mean mode number $\langle N(E) \rangle$ even down to the lowest eigenvalues. For $E \geq 75$ the staircase function lies under the curve corresponding to the asymptotic law eq. (24). The reason is that by using a limited

Table 1
Upper bounds for the first ten energies

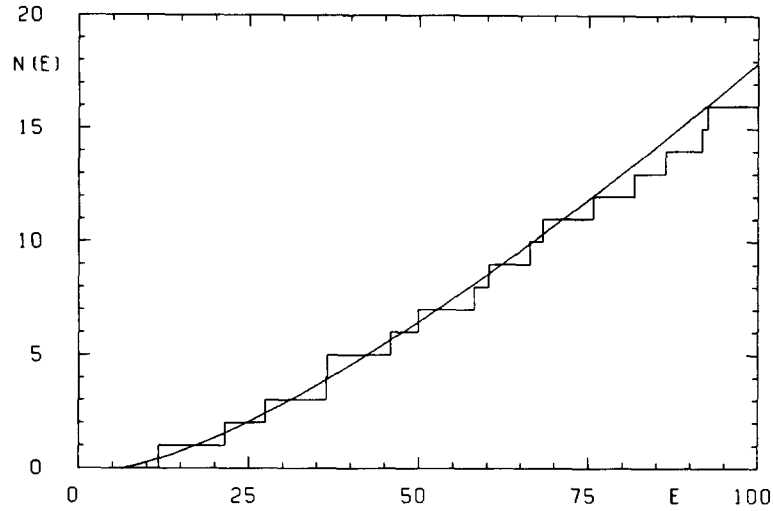| n	1	2	3	4	5	6	7	8	9	10
E_n	11.74	21.46	27.4	3(.3	36.5	45.8	49.8	58.1	60.2	66.2

Fig. 6. Staircase function $N(E)$ in comparison with the asymptotic law eq. (24).

number of functions $\varphi_m(\eta, \xi)$ "too high" upper bounds for the higher eigenvalues are obtained from the variational principle.

4. Periodic-orbit theory

4.1. Hyperbola billiard

The periodic-orbit theory usually is presented in form of a semiclassical approximation ($\hbar \to 0$) for the trace of the energy-dependent Green's function (resolvent),

$$g(E) := \mathrm{Tr}\left(\frac{1}{E - \hat{H}}\right) = \sum_n \frac{1}{E - E_n}, \tag{25}$$

where $\hat{H}$ is the Hamiltonian and E_n are its eigenvalues. In case of the hyperbola billiard this approximation is given by

$$g(E) = g_0(E) - \frac{\mathrm{i}}{\hbar} \sum_\gamma \sum_{k=1}^\infty \frac{m l_\gamma}{p} \frac{(-1)^{k n_\gamma} \exp(\mathrm{i} k p l_\gamma / \hbar)}{\exp(k u_\gamma / 2) - (-1)^{k n_\gamma} \exp(-k u_\gamma / 2)}, \tag{26}$$

where $p = \sqrt{2mE}$ denotes the momentum. The sum over γ runs over all primitive periodic orbits γ, and k is the number of their multiple traversals. l_γ is the length of the orbit γ and u_γ is its instability exponent. u_γ and the Lyapunov exponent λ_γ are related by $u_\gamma = \lambda_\gamma l_\gamma m / p$. n_γ is the number of reflections on the boundary for one traversal of the periodic orbit. If an orbit γ is described by a ternary sequence that consists of N letters, then $n_\gamma = 2N + N_b$, where N_b is the number of letters "b" in the sequence. $g_0(E)$ is the contribution of the so-called "zero-length orbits" and corresponds to the Thomas–Fermi approximation.

In ref. [10] we presented for the first time generalized versions of the periodic-orbit sum rule, eq. (26), which involve absolutely convergent series only. These sum rules represent a semiclassical approximation to a generalized sum over the energy eigenvalues, $\sum_n h(p_n)$, $p_n = \sqrt{2mE_n}$, involving a "smearing function" $h(p)$ which has to satisfy certain conditions in order to ensure convergence. Depending on the kind of application there are many possibilities for a useful choice of the function $h(p)$. Various examples are given in ref. [8]. In order to determine the energy eigenvalues we found most useful the choice of a Gaussian smearing function in case of which the *periodic-orbit sum rule* takes the form

$$d_\varepsilon(E) := \sum_n \left[\exp\left(- \frac{(p - p_n)^2}{\varepsilon^2} \right) + \exp\left(- \frac{(p + p_n)^2}{\varepsilon^2} \right) \right]$$

$$= \int_0^\infty dp' \left[\exp\left(- \frac{(p - p')^2}{\varepsilon^2} \right) + \exp\left(- \frac{(p + p')^2}{\varepsilon^2} \right) \right] \bar{d}(p')$$

$$+ \frac{\varepsilon}{\sqrt{\pi}\, \hbar} \sum_\gamma \sum_{k=1}^\infty \frac{l_\gamma(-1)^{kn_\gamma} \cos(kpl_\gamma/\hbar)}{\exp(ku_\gamma/2) - (-1)^{kn_\gamma} \exp(-ku_\gamma/2)} \exp\left(- \frac{\varepsilon^2 k^2 l_\gamma^2}{4\hbar^2} \right), \tag{27}$$

where

$$\bar{d}(p) := \frac{p}{m} \frac{d}{dE} \langle N(E) \rangle, \quad E = \frac{p^2}{2m}.$$

According to our results in section 3, $\langle N(E) \rangle$ can be identified with the asymptotic law (24). Here $\varepsilon > 0$ is a smearing parameter that can be chosen arbitrarily. The exponential term at the end of eq. (27) leads to a very strong damping of the contribution of orbits with large lengths. The smaller ε is chosen the smaller is the width of the Gaussian peaks at the momenta p_n, but the larger is the number of orbits that give a significant contribution to the periodic-orbit sum.

In figs. 7a and 7b we show the Gaussian level density eq. (27) for $\varepsilon = 0.2$ as a function of the energy E (in our numerical evaluations we use the following units: $\hbar = 2m = 1$). The full line represents the right-hand side of eq. (27) taking into account all periodic orbits with $N \leq 3$ and $N \leq 5$, respectively. The
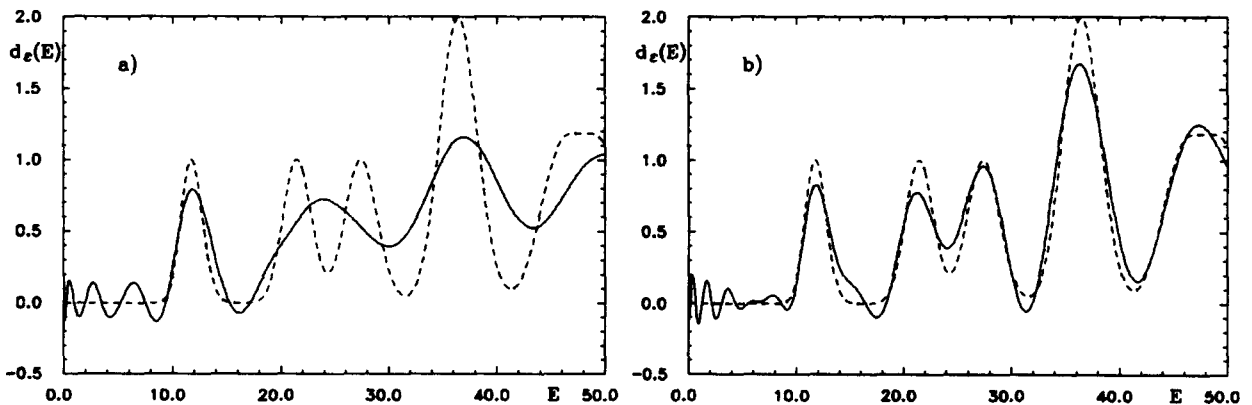

Fig. 7. Gaussian smoothed energy-level density $d_\varepsilon(E)$ for $\varepsilon = 0.2$ including all orbits with (a) $N \leq 3$ and (b) $N \leq 5$; (full line) calculated from periodic orbits, (dashed line) calculated from our numerical solution of the Schrödinger equation.

dashed line corresponds to the left-hand side of eq. (27) calculated from the first 10 approximate energy eigenvalues. In fig. 7b the agreement between both lines is surprisingly good in view of the small number of summed orbits. Even for the ground state energy the periodic-orbit theory gives an excellent approximation despite its semiclassical nature.

In figs. 8a and 8b the Gaussian level density is shown for $\varepsilon = 0.1$ in a larger range of the energy E. Again the full line represents the sum over the periodic orbits whereas the dashed line is calculated from the approximate quantum-mechanical energies. The periodic-orbit sums were evaluated using all orbits with $N \leq 9$ (fig. 8a) and $N \leq 14$ (fig. 8b). This corresponds to a contribution of 1061 and 136 699 different lengths respectively. As can be seen the agreement between the dashed and the full line improves only slowly.

The number of orbits that have to be taken into account in the periodic-orbit sum in order to resolve a momentum difference Δp can be estimated from the fact that each orbit γ contributes an oscillation to the smeared spectral density which has a "wavelength" $\Delta p \sim 2\pi\hbar/l_\gamma$. This implies that in order to resolve Δp one has to sum over all orbits with length $l_\gamma \lesssim 2\pi\hbar/\Delta p$. From the exponential increase of the number $\mathcal{N}(l)$ of orbits with length $l_\gamma \leq l$ then follows that a resolution of $\Delta p/2$ requires the summation over the square of the number of orbits that are needed in order to resolve Δp.

4.2. Desymmetrized hyperbola billiards

Symmetries of a system can be used in order to essentially increase the energy resolution of the periodic-orbit theory. The hyperbola billiard system is invariant under a geometrical reflection on the straight line $y = x$. For this reason it is possible to find a basis of eigenfunctions of the Hamiltonian $\hat{H}$ that are either odd or even functions with respect to this reflection. The even eigenfunctions satisfy Neumann boundary conditions on the line $y = x$, whereas the odd eigenfunctions satisfy Dirichlet boundary conditions on this line. The periodic-orbit theory can be applied to both classes of eigenfunctions separately.

Dirichlet boundary conditions: In order to determine the eigenvalues of the odd eigenfunctions one has to apply the periodic-orbit theory to one half of the billiard system, e.g. to that system which is bounded by the x-axis, the hyperbola $y = 1/x$ and the straight line $y = x$. The periodic orbits for this system can be determined from the periodic orbits of the whole system according to the following rules. To each periodic orbit of the original system can be associated a periodic orbit of the new desymmetrized system.
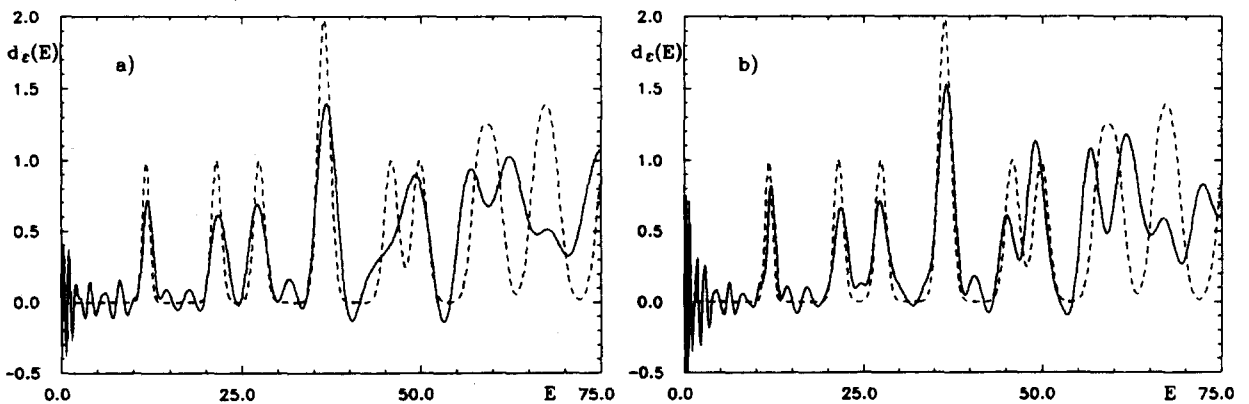

Fig. 8. Gaussian smoothed energy-level density $d_\varepsilon(E)$ for $\varepsilon = 0.1$ including all orbits with (a) $N \leq 9$ and (b) $N \leq 14$.

The only exception is that periodic orbit which runs along the line $y = x$ for which no corresponding orbit in the desymmetrized billiard exists. If an orbit which is described by a sequence "a" is not invariant under reflection on the symmetry line $y = x$ ($Ra \neq a$) then it is mapped onto an orbit in the desymmetrized system which has the same length, the same instability exponent and the same sign-factor $(-1)^{n_\gamma}$. The reflected orbit which is described by the sequence Ra is mapped onto the same orbit in half of the area. For this reason the multiplicity of the corresponding symmetry class is halved. On the other hand, orbits which have the symmetry property $a \equiv Ra$ are mapped onto orbits in half of the area that have half of the length and half of the instability exponent. The sign factor of the orbit in the desymmetrized billiard is $(-1)^{1+N_b/2}$, where N_b is the number of letters "b" in the sequence "a".

Neumann boundary conditions: The periodic-orbit theory can also be applied to the eigenvalues of the even eigenfunctions that satisfy Neumann boundary conditions on the line $y = x$. For that purpose again the periodic orbits for half of the area are needed, this time including the periodic orbit along the line $y = x$. The difference is the number n_γ in the numerator of eq. (27), which now does not count all reflections on the boundary along one traversal of the periodic orbit but only those reflections that do not take place on the line $y = x$. There is a simple rule relating the sign factor $(-1)^{n_\gamma}$ for the Neumann case to that for the Dirichlet case. For orbits to which correspond orbits with $Ra \neq a$ in the whole area both factors are equal. In the other case ($Ra \equiv a$) the sign factors have opposite sign. The number n_γ in the denominator of eq. (27) is the same as in the Dirichlet case.

In figs. 9a to 9c the smeared spectral density is shown for $\varepsilon = 0.2$ for odd and even eigenfunctions together and for both classes of eigenfunctions separately. In the periodic orbit sums all orbits were taken into account which are reflected at most seven times on the hyperbola. As can be seen, the energy resolution in figs. 9b and 9c is significantly improved in comparison with fig. 9a. The first ten energy eigenvalues of the whole hyperbola billiard that can be read off from these figures are listed in table 2. E_2, E_4, E_7 and E_9 are eigenvalues of odd wave functions, the other energies are eigenvalues of even wave functions. The values in table 2 are in good agreement with the values in table 1 except for E_8 and E_{10}, which are probably more accurate than the values obtained from the variational principle.

5. Conclusions

We have shown in this paper how the periodic orbits of the hyperbola billiard can be effectively represented by a ternary code, how the multiplicities of the periodic orbits can be understood in terms of their symmetry properties, and how the lengths of the periodic orbits together with their instability exponents can be calculated with high precision using an extremum principle. Based on these results, we were able to determine more than 500 000 primitive periodic orbits. This large sample of orbits made it possible to study detailed properties of the length spectrum of the periodic orbits. The main conclusion to be drawn from these studies is that the length spectrum behaves as if it would result from a random-walk process. The statistical distribution of lengths of periodic orbits which are reflected N times on the hyperbola $y = 1/x$, can be imagined for large enough N as result of a one-dimensional process consisting of N steps where each step is carried out in average with a constant mean-free path of length $\bar{l}$ and standard deviation σ. To show that this interpretation makes sense, we have calculated the length spacings distribution. Our numerical results are in nice agreement with a Poisson distribution, which is expected if the lengths are uncorrelated. From the random-walk model for the periodic orbits we were able to derive asymptotically for large lengths the famous exponential law for the periodic orbit number $\mathcal{N}(l)$ expected for strongly chaotic systems and thereby obtained a novel formula for the
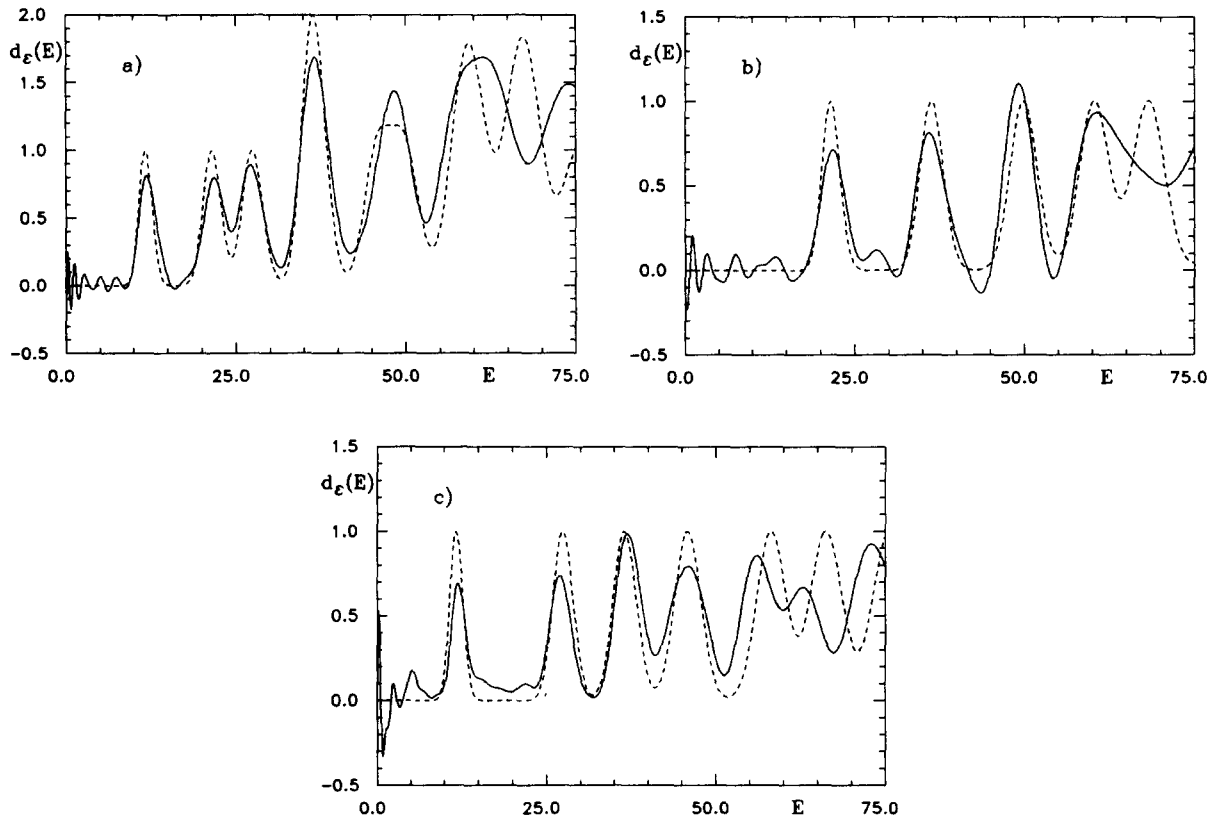
Fig. 9. Gaussian smoothed energy-level density $d_\varepsilon(E)$ for $\varepsilon = 0.2$ including all orbits with $N \leq 7$ for (a) odd and even wave functions, (b) odd wave functions and (c) even wave functions.

topological entropy which expresses its value in terms of the random-walk parameters $\bar{l}$ and σ and the number $\log 3$, the latter being a trace of the fact that the orbits are governed by a ternary code.

It is tempting to make the hypothesis that the properties of the periodic orbits, which we discovered in the special system of the hyperbola billiard, are found to hold also in other chaotic systems. It would be interesting to look for such properties in other non-integrable systems and to compare them with the results obtained for integrable systems.

It is notoriously difficult to determine the quantal energies from a numerical solution of the Schrödinger equation for classically chaotic systems, even on a large computer. To gain first information on the lowest energy levels of the hyperbola billiard, we have employed a variational method. A comparison with the modified Weyl's law indicates that the first ten eigenvalues should be not too bad an

Table 2
Approximate values for the first ten energies obtained from the periodic-orbit theory

n	1	2	3	4	5	6	7	8	9	10
E_n	12.0	21.7	27.0	36.0	37.0	45.9	49.2	55.9	60.7	63.0

approximation to the true quantal energies. To obtain more than ten eigenvalues with reasonable accuracy requires a more sophisticated method like, for example, Heller's method [11]. Computations using the latter method are presently carried out and results will be published elsewhere. It is hoped that the more elaborate methods will give us more eigenvalues with better accuracy and thus will allow us to study the energy level statistics.

In section 4 we have carried out a quantitative analysis of Gutzwiller's periodic-orbit theory. Since the original version of the periodic-orbit theory, i.e. the representation (26) for the trace of the Green's function, is at best conditionally convergent, we have based our analysis on the Gaussian smeared periodic-orbit sum rule (27), which is absolutely convergent for any smearing parameter $\varepsilon > 0$. Working with a convergent form of the periodic-orbit theory is of crucial importance in view of the limited number of classical orbits. Using a relatively large smearing parameter, i.e. $\varepsilon = 0.2$, it turned out that the periodic-orbit theory evaluated with only 36 terms agrees at low energies surprisingly well with the "true" Gaussian level density obtained from a numerical solution of the Schrödinger equation (see fig. 7b). If, however, the energy resolution is improved by taking $\varepsilon = 0.1$, one requires all available 136 699 terms in order to be able to distinguish between the energy levels E_6 and E_7 (see fig. 8b).

In section 4.2 we have shown that the energy resolution is significantly improved if the periodic-orbit theory is applied to the desymmetrized billiard systems instead to the full hyperbola billiard. Summarizing the results of section 4, we can say that the periodic-orbit theory provides indeed a substitute for the semiclassical quantization rules for our strongly chaotic system. In contrast to what one might have expected, the theory works quite well at low energies, while in the genuine semiclassical region, i.e. at large energies, much more periodic orbits would be needed than have been calculated in this paper. There remains the challenge to invent a powerful summation method to handle a huge number of periodic orbits in the periodic-orbit sum.

Acknowledgements

Appendix A. Extremum principle for periodic orbits

Suppose $P_{i-1}(x_{i-1}|1/x_{i-1})$, $P_i(x_i|1/x_i)$ and $P_{i+1}(x_{i+1}|1/x_{i+1})$ are three successive points of a periodic orbit on the hyperbola. The lengths of the segments of the periodic orbit from P_{i-1} to P_i and from P_i to P_{i+1} are denoted by $l_{i-1,i}$ and $l_{i,i+1}$ respectively. P'_{i-1} and P'_{i+1} are two points that are obtained by extending the two line segments of the orbit that have P_i as common point until they hit one of the hyperbolas $y = 1/x$ or $y = -1/x$ (see fig. 10). Now consider an ellipse through P_i with foci P'_{i-1} and P'_{i+1}. Because of the focal property of the ellipse that the lines $P'_{i-1}P_i$ and $P'_{i+1}P_i$ form equal angles with the tangent to the ellipse at point P_i it follows that the ellipse and the hyperbola have a common tangent at point P_i. It further holds that $l_{i-1,i} + l_{i,i+1} = A$, where A is the major axis of the ellipse. If now the position of the point P_i on the hyperbola is changed one sees immediately that the major axis of the ellipse through P_i with foci P'_{i-1} and P'_{i+1} is increased and therefore also the sum of the distances $\overline{P'_{i-1}P_i}$ and $\overline{P_iP'_{i+1}}$. Since this argument holds for every point of the periodic orbit on the hyperbola, the following *extremum principle for periodic orbits* is obtained:

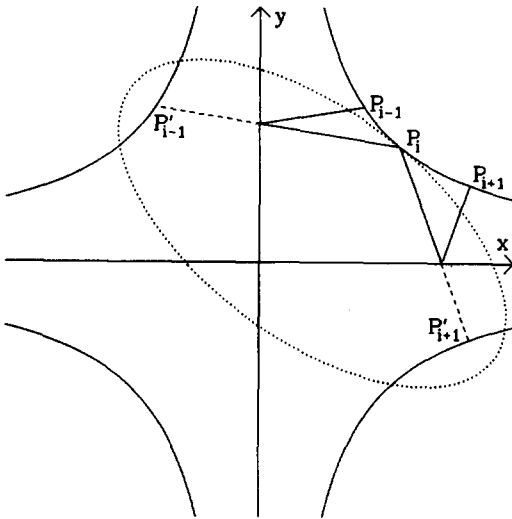$$\frac{\partial}{\partial x_i}L(x_1,\ldots,x_N) = 0 \quad \forall i = 1,\ldots,N, \tag{A.1}$$

Fig. 10. Illustration of the extremum principle.

and

$$\frac{\partial^2}{\partial x_i^2} L(x_1,\ldots,x_N) > 0 \quad \forall i = 1,\ldots,N, \tag{A.2}$$

where L is the length of a given periodic orbit as a function of its N points on the hyperbola, i.e.

$$L(x_1,\ldots,x_N) = \sum_{i=1}^{N} L_i(x_i,x_{i+1}), \quad x_{N+1} := x_1. \tag{A.3}$$

There are three different possibilities for the functional dependence of the length $L_i(x_i, x_{i+1})$ of the segment of the orbit from $P_i(x_i|1/x_i)$ to $P_{i+1}(x_{i+1}|1/x_{i+1})$:

$$L_i(x_i,x_{i+1}) = f_x(x_i,x_{i+1}) := \left[(x_i - x_{i+1})^2 + (1/x_i + 1/x_{i+1})^2\right]^{1/2},$$

$$= f_y(x_i,x_{i+1}) := \left[(x_i + x_{i+1})^2 + (1/x_i - 1/x_{i+1})^2\right]^{1/2},$$

$$= f_b(x_i,x_{i+1}) := \left[(x_i + x_{i+1})^2 + (1/x_i + 1/x_{i+1})^2\right]^{1/2}. \tag{A.4}$$

These three cases correspond to segments in which there is a reflection on the x-axis only or on the y-axis only or on both axes respectively. Thus if the given periodic orbit is represented by the ternary

sequence $a = (a_1, \ldots, a_N)$ (see section 2.1), its length function reads

$$L(x_1, \ldots, x_N) = \sum_{i=1}^{N} f_{a_i}(x_i, x_{i+1}). \tag{A.5}$$

Appendix B. Calculation of the monodromy matrix

Consider a certain periodic orbit. In its vicinity a coordinate system can be introduced whose x-coordinate is parallel to the orbit and whose y-coordinate is perpendicular to it. A particle that starts at $r = (x_0, dy)$ with momentum $p = (p_x, dp_y)$ infinitesimally close to the periodic trajectory will have after one traversal the coordinates $r' = (x_0, dy')$ and momentum $p' = (p_x, dp'_y)$. The monodromy matrix M of the periodic orbit is then defined by

$$\begin{pmatrix} dy' \\ dp'_y \end{pmatrix} = M \begin{pmatrix} dy \\ dp_y \end{pmatrix}. \tag{B.1}$$

It has the property $\det M = 1$. Introducing an angle α between momentum direction and x-direction one obtains

$$\begin{pmatrix} dy' \\ d\alpha' \end{pmatrix} = \tilde{M} \begin{pmatrix} dy \\ d\alpha \end{pmatrix}, \qquad \tilde{M} = \begin{pmatrix} M_{11} & pM_{12} \\ (1/p)M_{21} & M_{22} \end{pmatrix}, \quad p = |p|. \tag{B.2}$$

The matrix $\tilde{M}$ can be decomposed into partial matrices $\tilde{M}_i$

$$\tilde{M} = \tilde{M}_{i\,\text{max}} \cdot \ldots \cdot \tilde{M}_2 \cdot \tilde{M}_1. \tag{B.3}$$

This is done by traversing the periodic orbit once and inserting into the product one matrix $\tilde{M}_i$ for every straight line segment and for every reflection on the boundary. It follows from geometrical considerations that for a straight line segment the matrix $\tilde{M}_i$ is of the form

$$\tilde{M}_i = \begin{pmatrix} 1 & l_i \\ 0 & 1 \end{pmatrix}, \tag{B.4}$$

where l_i is the length of the line segment. For a reflection on the boundary the corresponding matrix $\tilde{M}_i$ has the form

$$\tilde{M}_i = \begin{pmatrix} -1 & 0 \\ 2/(R_i \cos \beta_i) & -1 \end{pmatrix}. \tag{B.5}$$

Here β_i is the angle between the incoming trajectory and the normal to the boundary. R_i is the radius of curvature of the boundary at the collision point. R_i is greater than zero if the boundary is convex and it is less than zero if the boundary is concave. If the reflection takes place on a straight line, $R_i = \infty$.

In case $|\text{Tr}\,M| > 2$, the periodic orbit is unstable and M has eigenvalues $\Lambda_{1,2} = e^{\pm u}$ or $\Lambda_{1,2} = -e^{\pm u}$, where $u > 0$ is the instability exponent. The Lyapunov exponent λ of an unstable periodic orbit is in our

case defined as $\lambda = u/T$, where T is the period of the periodic orbit. If $|\mathrm{Tr}\, M| < 2$, the periodic orbit is stable and M has eigenvalues $\Lambda_{1,2} = \mathrm{e}^{\pm iv}$, where v is the angle of stability.

For billiards whose boundaries consist of concave and straight pieces only and which have the property that every classical trajectory is reflected from a concave part of the boundary at least once it is easy to show that the product of matrices $\tilde{M} = \tilde{M}_{i\,\mathrm{max}} \cdot \ldots \cdot \tilde{M}_1$ satisfies the relation $|\mathrm{Tr}\, \tilde{M}| > 2$. For that reason all periodic orbits of the hyperbola billiard are unstable and have positive instability exponents.

Note added in proof

After submission of this paper we have used an improved method to calculate the eigenvalues of the Schrödinger equation, which allows us to consider also higher excited states and to study the level statistics. The nearest-neighbour spacing distributions for the two symmetry classes are in agreement with the GDE predictions of random-matrix theory. Details will be given in a forthcoming DESY preprint.

References

[1] M.C. Gutzwiller, J. Math. Phys. 8 (1967) 1979; 10 (1969) 1004; 11 (1970) 1791; 12 (1971) 343; in: Path Integrals and their Applications in Quantum, Statistical and Solid-State Physics, eds. G.J. Papadopoulos and J.T. Devreese (Plenum, New York, 1978) p. 163; Physica D 7 (1983) 341.
[2] R. Balian and C. Bloch, Ann. Phys. (NY) 69 (1972) 76; 85 (1974) 514;
    R. Dashen, B. Hasslacher and A. Neveu, Phys. Rev. D 10 (1974) 4114;
    M.V. Berry, in: Semiclassical Mechanics of Regular and Irregular Motion, Proceedings of the Les Houches Summer School Session XXXVI, eds. G. Iooss, R.H.G. Helleman and R. Stora (North-Holland, Amsterdam, 1983) p. 171; Proc. R. Soc. London Ser. A 400 (1985) 229; A 413 (1987) 183;
    A. Voros, J. Phys. A 21 (1988) 685.
[3] E. Bogomolny, Physica D 31 (1988) 169; JETP Lett. 47 (1988) 526;
    M.V. Berry, Proc. R. Soc. London Ser. A 423 (1989) 219.
[4] M.C. Gutzwiller, J. Math. Phys. 12 (1971) 343; 14 (1973) 139; 18 (1977) 806; Phys. Rev. Lett. 45 (1980) 150; Physica D 5 (1982) 183; J. Phys. Chem. 92 (1988) 3154; ITP University of Santa Barbara preprint NSF-ITP-89-90i.
[5] M. Tabor, Physica D 6 (1983) 195;
    M.L. Du and J.B. Delos, Phys. Rev. Lett. 58 (1987) 1731;
    D. Wintgen and H. Friedrich, Phys. Rev. A 36 (1987) 131;
    D. Wintgen, Phys. Rev. Lett. 58 (1987) 1589; 61 (1988) 1803;
    P. Cvitanović and B. Eckhardt, ITP University of Santa Barbara preprint NSF-ITP-89-24i;
    J. Keating, Ph.D. Thesis, University of Bristol (May 1989).
[6] J. Hadamard, J. Math. Pures Appl. 4 (1898) 27;
    M.C. Gutzwiller, Phys. Rev. Lett. 45 (1980) 150; Phys. Scr. T9 (1985) 184; Contemp. Math. 53 (1986) 215.
[7] R. Aurich and F. Steiner, Physica D 32 (1988) 451.
[8] R. Aurich, M. Sieber and F. Steiner, Phys. Rev. Lett. 61 (1988) 483;
    R. Aurich and F. Steiner, Physica D 39 (1989) 169.
[9] B. Simon, J. Func. Anal. 53 (1983) 84;
    F. Steiner and P. Trillenberg, DESY preprint 89-036; J. Math. Phys., in press.
[10] M. Sieber and F. Steiner, Phys. Lett. A144 (1990) 159.
[11] E. Heller, private communication.